Nuclear Instruments and Methods in Physics Research A 680 (2012) 97–102

Contents lists available at SciVerse ScienceDirect

Nuclear Instruments and Methods in Physics Research A

journal homepage: www.elsevier.com/locate/nima

Nuclear reactor pulse tracing using a CdZnTe electro-optic radiation detector

Kyle A. Nelson [a,*], Jeffrey A. Geuther [b], James L. Neihart [a], Todd A. Riedel [a], Ronald A. Rojeski [c], Philip B. Ugorowski [a], Douglas S. McGregor [a]

[a] S.M.A.R.T. Laboratory, Mechanical and Nuclear Engineering, Kansas State University, Manhattan KS 66506, USA
[b] TRIGA Mark II Nuclear Reactor, Mechanical and Nuclear Engineering, Kansas State University, Manhattan KS 66506, USA
[c] Nanometrics, Inc., 1550 Buckeye Drive, Milpitas CA 95035, USA

ARTICLE INFO

Article history:
Received 5 July 2011
Received in revised form
22 February 2012
Accepted 27 February 2012
Available online 6 April 2012

Keywords:
Pockels cell
Reactor pulsing
Radiation detector

ABSTRACT

CdZnTe has previously been shown to operate as an electro-optic radiation detector by utilizing the Pockels effect to measure steady-state nuclear reactor power levels. In the present work, the detector response to reactor power excursion experiments was investigated. Peak power levels during an excursion were predicted to be between 965 MW and 1009 MW using the Fuchs–Nordheim and Fuchs–Hansen models and confirmed with experimental data from the Kansas State University TRIGA Mark II nuclear reactor. The experimental arrangement of the Pockels cell detector includes collimated laser light passing through a transparent birefringent crystal, located between crossed polarizers, and focused upon a photodiode. The birefringent crystal, CdZnTe in this case, is placed in a neutron beam emanating from a nuclear reactor beam port. After obtaining the voltage-dependent Pockels characteristic response curve with a photodiode, neutron measurements were conducted from reactor pulses with the Pockels cell set at the 1/4 and 3/4 wave bias voltages. The detector responses to nuclear reactor pulses were recorded in real-time using data logging electronics, each showing a sharp increase in photodiode current for the 1/4 wave bias, and a sharp decrease in photodiode current for the 3/4 wave bias. The polarizers were readjusted to equal angles in which the maximum light transmission occurred at 0 V bias, thereby, inverting the detector response to reactor pulses. A high sample rate oscilloscope was also used to more accurately measure the FWHM of the pulse from the electro-optic detector, 64 ms, and is compared to the experimentally obtained FWHM of 16.0 ms obtained with the ^{10}B-lined counter.

1. Introduction

The electro-optic (EO) radiation detector, a new category of detector, has the unique ability to detect radiation with no signal processing equipment connected to the sensor [1]. The EO detector utilizes the Pockels effect, which involves the passing of collimated laser light through a transparent birefringent crystal, positioned between crossed polarizers, and focused upon a photodiode. The Pockels cell setup utilizing crossed polarizers, oriented 90° to one another, is referred to here as the 'standard' Pockels cell arrangement. Applying a voltage bias to the crystal will change its refractive index and, therefore, alter the polarization of the light propagating through the second polarizer, also known as the analyzer, and eventually the photodiode current output. Radiation interactions occurring in the crystal will generate free electrical charges, which can perturb the electric field of the crystal and cause a change in the state of polarization. This change in electric field will alter the amount of light transmitted through the analyzer and, consequently, the current (or voltage) output of the photodiode.

The electric field distribution within the Pockels cell is a function of the electrode dimensions. For instance, a voltage placed across an ideal planar device would have equal charge densities of opposite sign upon the contacts; hence the electric field would be constant across the device. However, a Pockels cell with a small dot-shaped contact opposing a large planar contact upon the other surface, having the same number of charges on each contact, would consequently cause the charge density of the small contact to be larger than that of the large contact, and thereby, cause the electric field near the small contact to be much higher than the electric field adjacent the large contact. The effect can be manipulated to enhance the change in photodiode current output from radiation interactions in the Pockels cell crystal by collimating the laser light through the high electric field region of the Pockels cell [1]. The result is a greater change in current output at the photodiode than for a uniform field [1]. The conceptual setup for a 'dot' contact, an optimum anode geometry for electric field enhancement, is shown in Fig. 1. Because CdZnTe was demonstrated as a viable EO detector, mainly due to the

* Corresponding author.
E-mail addresses: nuclearengg@gmail.com, knelson1@ksu.edu (K.A. Nelson).

0168-9002/$ - see front matter © 2012 Elsevier B.V. All rights reserved.
http://dx.doi.org/10.1016/j.nima.2012.02.048

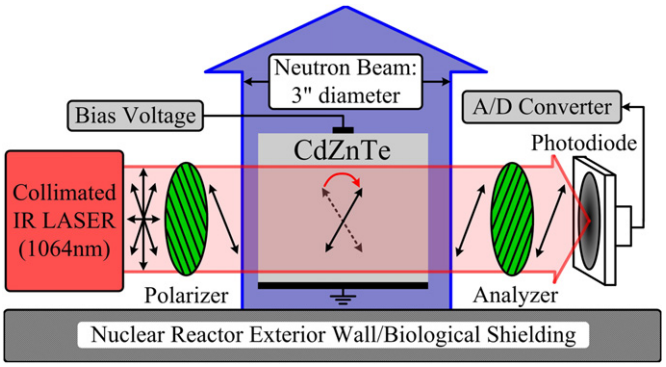

Fig. 1. Depiction of the Pockels cell experimental arrangement in the radial neutron beam.

relatively long free carrier lifetimes (compared to most EO crystals) and the $^{113}Cd(n,\gamma)^{114}Cd$ neutron reaction, the same experimental configuration used for steady neutron monitoring [1] was used for the reactor pulsing measurements.

The Kansas State University (KSU) TRIGA* Mark II nuclear reactor can be "pulsed", by withdrawing the three standard control rods to attain criticality at 10 W and afterwards ejecting the transient control rod. By ejecting the transient control rod pneumatically, a rapid upward spike in reactor power is observed, reaching approximately 1 GW of thermal power with a pulse full width half maximum (FWHM) of approximately 16.0 ms. Using a data recording system, the reactor pulses were measured in real time at the 1/4 and 3/4 wave bias settings of the characteristic Pockels curve for the standard Pockels cell configuration. Afterwards, the measurements were performed with the polarizer and analyzer set to equal angles, instead of the typical 90° orientation. This alternative arrangement, referred to as the "inverted" Pockels cell configuration, causes an inversion of the characteristic Pockels curve, and consequently, causes the maximum light transmission to occur at 0 V bias. Reactor pulsing was repeated at the same bias settings as the standard Pockels cell assembly for the inverted configuration.

2. Theoretical considerations

2.1. Pockels effect

The intensity of transmitted light through a Pockels cell is a function of the applied electric field,

$$I = I_o \sin^2\left(\frac{\pi n_o^3 r d}{\lambda} E\right) \tag{1}$$

where I_0 is the maximum light intensity transmitted through uncrossed polarizers, n_o is the zero bias refractive index, r is the Pockels electro-optic coefficient for the crystal, d is the path length of light transmitted through the crystal, λ is the wavelength of incident light, E is the electric field perpendicular to the optical path and I is the transmitted light [2]. The maximum change of light intensity per unit applied potential can be found by analyzing the second derivative of Eq. (1), which indicates that the largest intensity change occurs at the 1/4 and 3/4 wave positions and optimal operational settings.

^{113}Cd has a thermal neutron capture cross section of 20,000 b with a natural abundance of 12%, [3–5]. The neutron reaction of interest in the present work is [4,6,7],

$$^{113}Cd + n \rightarrow {}^{114}Cd + \gamma_1(558.6\ \text{keV}) + \gamma_2(651.3\ \text{keV}) + \gamma\text{'s}, \tag{2}$$

The reaction products, when absorbed in the Pockels cell, create ionization charge clouds. The application of a bias voltage across the Pockels cell can cause these free charges to drift to their respective electrodes (electrons to the anode, holes to the cathode), and by doing so create a smaller internal electric field opposing the externally applied electric field. This change in the Pockels cell electric field will also alter the polarization of light passing through the cell. Consequently, the amount of light passing through the second polarizer, or analyzer, will also change, which can be detected by a photodiode placed beyond the radiation field.

2.2. Reactor power excursion

The TRIGA Mark II nuclear reactor, designed as a training reactor, has the ability to perform reactor power excursion experiments, i.e., reactor pulsing. In other words, the reactor has the ability to release a large amount of fission neutrons and energy over a short period of time. TRIGA reactor pulse experiments and empirical calculations have been performed extensively and reported by Stone, et al. [8]. A majority of the pulse occurs in less than one second; typically the FWHM of the pulse is approximately 20 ms and dependent on the size of the pulse. In general, the FWHM of the pulse decreases as the peak power, or reactivity inserted, increases.

The particular physical attribute of the fuel that allows pulsing to be possible is the prompt negative temperature coefficient of reactivity. The oscillations of the hydrogen atoms in the ZrH fuel matrix, an effect which increases rapidly with fuel temperature, results in the hardening of the neutron energy spectrum and a corresponding decrease in core reactivity [8–12]. The pulses are generated by ejecting a control rod, using air pressure, to rapidly insert >1 \$ of reactivity, causing the reactor to become prompt supercritical. In this state, the reactor power increases rapidly until the rise in fuel temperature causes the hydrogen atoms to oscillate rapidly. This adds sufficient negative reactivity to cause the reactor to become subcritical.

The power during a pulse in a TRIGA reactor can be modeled using either the Fuchs–Nordheim or Fuchs–Hansen models [13–16]. Both the Fuchs–Nordheim and Fuchs–Hansen models are briefly described below and used as theoretical benchmarks for the EO detector experiments and comparisons to TRIGA pulse data. For the Fuchs–Nordheim model, the power as a function of time, $P(t)_{FN}$, is shown in Eq. (3), and the FWHM of the pulse was obtained using Eq. (4). The maximum power, P_{max}, during a pulse can also be calculated using Eq. (5), assuming a constant K. However, the heat capacity, $C_p(t)$, in Eq. (3) uses the change in temperature over time, $T(t)$, to assist in calculating the power in Eq. (3) [see Eqs. (6) and (7)]. This is referred to as the 'modified' Fuchs–Nordheim model whereas the standard Fuchs–Nordheim model uses a ΔT in place of the $T(t)$ [9].

$$P(t)_{FN} = \frac{NC_p(t)\ (\rho_{FN}\beta)^2}{2\alpha l}\ \text{sech}^2\left(\frac{t\rho_{FN}\beta}{2l}\right) \tag{3}$$

$$\text{FWHM}_{FN} = \frac{3.525}{\omega} \tag{4}$$

$$P_{max} = \frac{(\rho_{FN}\beta)^2}{2\alpha K l} \tag{5}$$

$$C_p(t) = 805 + 1.65(T(t) - 25\,^\circ C) \tag{6}$$

$$T(t) = T_o + \frac{\int_0^t P(t)_{FN}\,dt}{C_p} \tag{7}$$

In the above equations, N is the number of fuel elements, β is the effective delayed neutron fraction, C_p is the heat capacity of each fuel element as a function of time shown in Eq. (6), ρ_{FN} is the

* Training, Research, Isotopes, General Atomics.

prompt reactivity inserted in the Fuchs–Nordheim equation, α is the prompt negative temperature coefficient of reactivity, and l is the prompt neutron lifetime. As mentioned previously, the heat capacity changes with temperature for the ZrH fuel matrix and the temperature changes in the reactor during a pulse. This effect was calculated using Eq. (7).

The power as a function of time, $P(t)_{FH}$, from the Fuchs–Hansen model is represented by Eq. (8) below where the constants A, c, γ, α_o, and b are also defined in Eqs. (9)–(13).

$$P(t)_{FH} = \frac{2c^2 A e^{-ct}}{b(1+Ae^{-ct})^2} \tag{8}$$

$$A \cong \frac{2\alpha_o^2}{bP_o} \tag{9}$$

$$c = \sqrt{\alpha_o^2 + 2bP_o} \tag{10}$$

$$\gamma = \frac{\alpha}{C_p} \tag{11}$$

$$\alpha_o = \rho_{FH}/l \tag{12}$$

$$b = \gamma/l \tag{13}$$

where ρ_{FH} is the prompt reactivity inserted for the Fuchs–Hansen model, γ is the energy feedback coefficient and is related to the negative prompt temperature coefficient, α, through Eq. (11). The peak power was calculated manually along with the FWHM using linear interpolation. The Fuchs–Nordheim model is set up that the peak power occurs at time $t=0$, making it convenient to solve mathematically for the FWHM and peak power, P_{max}. In the Fuchs–Hansen model, time $t=0$ corresponds to the moment the pulse rod begins the withdrawal process. Shown below in Table 1 are the values associated with the constants used for the Fuchs–Nordheim and Fuchs–Hansen models [12,17–19]. The peak power calculated with the modified Fuchs–Nordheim and Fuchs–Hansen models, for 1.5 $ of excess reactivity inserted, were 965 MW and 1009 MW. A FWHM of 13.1 ms was obtained from both models.

The pulse is measured experimentally using a ^{10}B-line counter placed in the bulk shield tank outside the reactor core. Experimental and simulated data shows that the detector is operating as a gamma-ray detector because the neutrons are being moderated to the point they are considered negligible, while the gamma-rays are less affected by the low-Z materials surrounding the core. Previously, the detector was located in the core and becoming saturated during large pulses, resulting in inaccurate measurements of the peak power. The new location of the detector gives an accurate measurement of the FWHM since the gamma-rays being measured are from fissions during the pulse and travel the speed of light.

3. Experimental procedure

A polished 2 mm × 10 mm × 10 mm CdZnTe crystal, with a 1.5 mm diameter Au anode centered on one of the 10 mm × 10 mm faces and a 10 mm × 10 mm Au cathode on the opposing face, was used as the Pockels cell crystal. The CdZnTe cell was mounted such that the 10 mm × 10 mm Au coated cathode was perpendicular to a 3 in. diameter neutron beam emanating from a radial port at the KSU TRIGA Mark II nuclear reactor. The equipment specifics and configuration are discussed in greater detail elsewhere [1], but the conceptual arrangement is shown in Fig. 1. The current from the photodiode was measured using a Keithley 6485 picoameter interfaced with a LabView data recording system sampling one measurement approximately every 10 ms. The entire assembly was fastened to an optical table, over which was attached a light-tight metal enclosure to prevent interference from ambient light and background electronic noise.

A Pockels cell characteristic curve was obtained by recording the current on the electrometer in 50 V increments, ranging from 0 to 1600 V. This procedure revealed the 1/4 and 3/4 wave voltage bias settings. The photodiode current was measured as a function of time with the KSU TRIGA Mark II nuclear reactor pulsed at each of the 1/4 and 3/4 wave bias settings. Afterwards, the polarizer and analyzer were set to equal angles to obtain the inverted characteristic Pockels curve over a range of 0 to 1600 V in 50 V increments. Again, the characteristic curve was used to obtain the 1/4 and 3/4 wave bias settings, and neutron measurements were conducted with the reactor pulsed at these bias voltages. The reactivity insertion was set to 1.50 $ for all pulses, thereby, generating 992 MW of thermal power with each pulse as measured by the ^{10}B-lined counter. The 1.50 $ is the amount of excess reactivity inserted above the delayed neutron fraction (1.0 $), thus the total reactivity inserted including the sub-prompt reactivity is 2.50 $.

Additionally, a characteristic Pockels curve was obtained for $LiNbO_3$, a well-known EO crystal. However, previous results indicated that the charge carrier lifetimes in $LiNbO_3$ are too short to cause a measureable perturbation in the electric field; hence failed to show the same effect as observed with the CdZnTe crystal [1]. The reactor was pulsed at the 1/4 wave bias setting in an attempt to increase the concentration of free charge carriers to cause a change in output current at the photodiode, in hopes that the increase would allow for a measureable result.

A borated high-density polyethylene (HDPE) and Pb shutter was used to block the neutron and gamma-ray beam during several pulses to ensure that the response was from radiation interactions in the Pockels cell and not from electronic noise or background interactions in the surrounding equipment. The pulse experiments were performed at the 1/4 wave bias setting for the standard Pockels cell configuration. Additionally, the experiment was repeated with the laser off, and no shutter, to ensure that radiation was not scattering off the crystal setup into the photodiode to cause the change in photodiode current.

Table 1
Constants used in the Fuchs–Nordheim (FN) and Fuchs–Hansen (FH) models.

Symbol	FN Model	FH Model	Description
ρ_o ($)	1.5	1.5	The excess reactivity inserted in units of dollars.
N	85	–	The number of fueld elements in the reactor core.
α	1.2×10^{-4}	–	The prompt negative temperature feedback coefficient.
l	39 μs	39 μs	The prompt neutron lifetime.
β	0.007	0.007	The effective delayed neutron fraction.
γ	–	1.4×10^{-9}	The energy feedback coefficient.
P_o	–	100 W	The initial reactor power prior to the pulse.

An additional experiment was performed by replacing the electrometer and LabView recording system with an Agilent Infiniium 54832D oscilloscope, having a maximum sampling rate of 4G Sample/s. The EO detector was switched into the standard configuration and biased at 715 V, within the 1/4 wave region. The reactor was pulsed and the oscilloscope recorded the EO detector response.

4. Experimental results

From the characteristic Pockels cell curves obtained for the standard and inverted configurations of the CdZnTe crystal, shown in Fig. 2, the 1/4 and 3/4 wave bias settings were found to be 600 V and 1450 V for the standard and 550 V and 1300 V for the inverted arrangements. The responses to reactor pulsing for the standard Pockels cell configurations are shown in Figs. 3 and 4, where the change in photodiode current at 600 V was +40 μA and −22 μA at 1450 V. The responses to reactor pulsing for the inverted Pockels cell configuration are shown in Figs. 5 and 6, where the change in photodiode current was −45 μA at 550 V and +25 μA at 1300 V. The additional experiments performed with either the borated HDPE/Pb shutter or laser powered off showed no change in photodiode current when the reactor was pulsed, thereby, indicating that the change in photodiode current was due to the EO effect in the CdZnTe device. The $LiNbO_3$ EO crystal showed no response to reactor pulsing, likely a result of the short lifetimes of the free carriers in the crystal, less than 1 ps. [20].

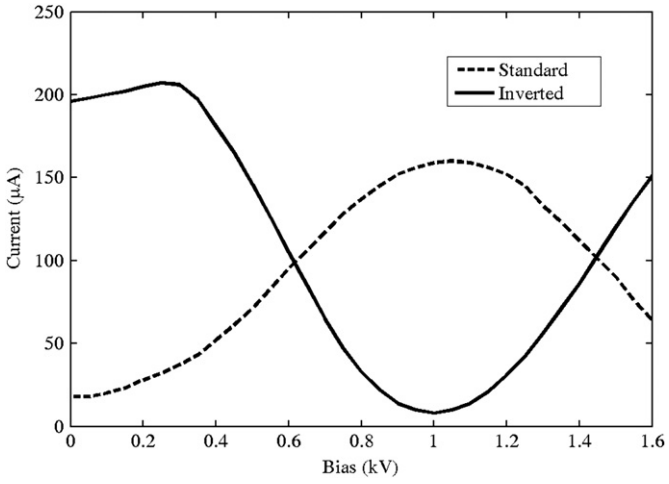

Fig. 2. The characteristic Pockels curves for the standard and inverted configurations.

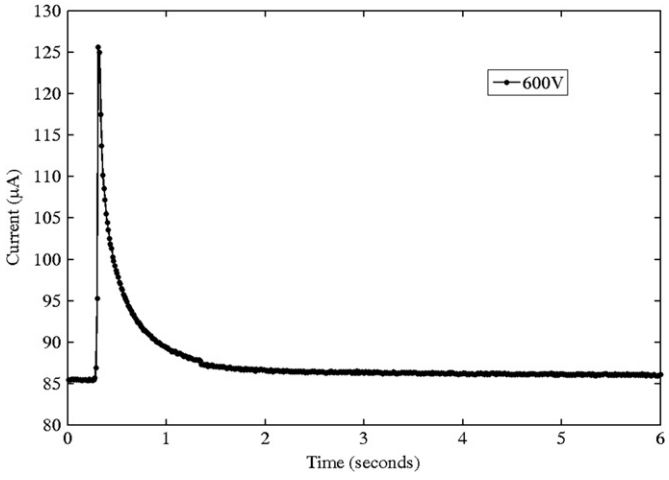

Fig. 3. The real time response of the CdZnTe EO detector to a reactor pulse using the standard Pockels cell configuration at the 1/4 wave bias (600 V).

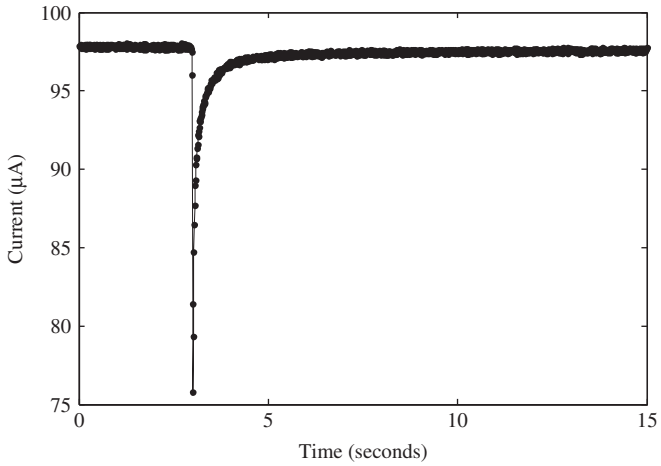

Fig. 4. The real time response of the CdZnTe EO detector to a reactor pulse using the standard Pockels cell configuration at the 3/4 wave bias (1450 V).

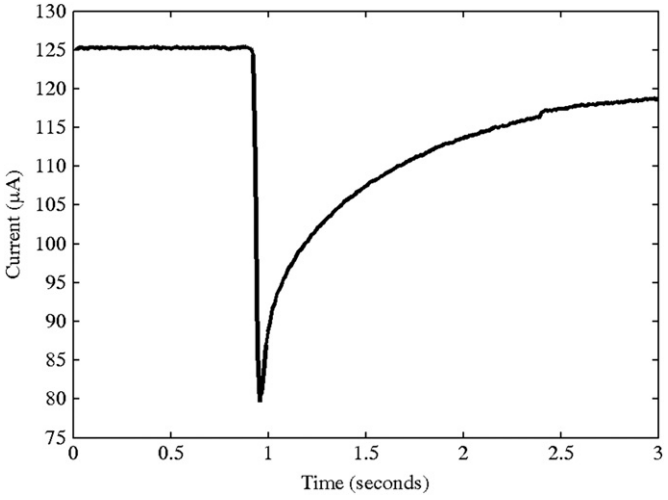

Fig. 5. The real time response of the CdZnTe EO detector to a reactor pulse using the inverted Pockels cell configuration at the 1/4 wave bias (550 V).

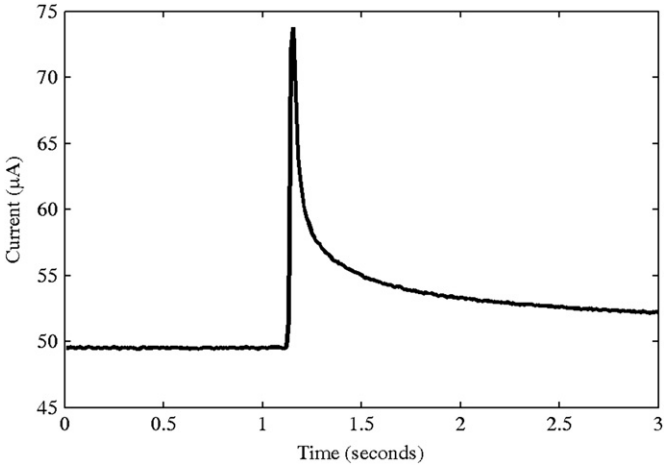

Fig. 6. The real time response of the CdZnTe EO detector to a reactor pulse using the inverted Pockels cell configuration at the 3/4 wave bias (1300 V).

The shape of the real time plot of the photodiode current for the CdZnTe EO crystal appears similar in shape to the theoretical results found by Stone, et al. [8]. The FWHM of the pulse in Fig. 3 is approximately 85 ms., more than four times longer than the theoretical 13.1 ms from the Fuchs–Nordheim and Fuchs–Hansen models or experimentally obtained 16.0 ms. FWHM of a reactor pulse. The FWHM of the pulse in Fig. 4, at the higher bias, is approximately 45 ms. The pulse response recorded with the Agilent oscilloscope is shown in Fig. 7, and has a FWHM of approximately 60 ms. Additionally, shown in Fig. 8 is a plot of the Fuchs–Hansen model with the EO detector response. The detector can be calibrated to measure the peak power for different reactivity insertions, but fails at predicting the FWHM [21]. Further, shown in Fig. 9 is the power as a function of time as calculated by the modified Fuchs–Nordheim, Eq. (3), and Fuchs–Hansen, Eq. (8), models and measured by the ^{10}B-lined detector. The peak power predicted by the Fuchs–Nordheim and Fuchs–Hansen models were 965 MW and 1009 MW, respectively.

5. Discussion

Because the slopes of the Pockels characteristic curve are opposite each other at the 1/4 and 3/4 wave bias settings, the changes in photodiode current should also be opposite to one another, a circumstance that also holds true for the inverted Pockels cell configuration. Comparing the changes in photodiode current at the 1/4 wave bias settings for the standard and inverted setups, the magnitudes are approximately the same, but the direction of the changes in photodiode current are opposite. This is consistent with the slopes being opposite at the 1/4 wave bias setting for the standard and inverted configurations. The effect was also observed for the 3/4 wave bias settings for each configuration, where the magnitudes of the changes in current are roughly the same, but opposite in direction. The fact that the current decreases for the 1/4 wave bias setting for the inverted configuration and increases for the 1/4 wave bias setting for the standard configuration further indicates that the photodiode current change is a result of the Pockels effect and not electronic noise, radiation background, or other effects.

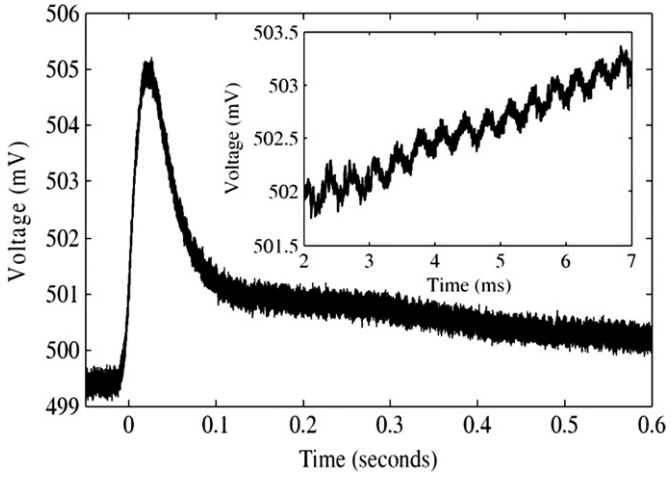

Fig. 7. The real time response of the CdZnTe EO detector to a reactor pulse using the standard Pockels cell configuration at the 1/4 wave bias (715 V) using a high sample rate oscilloscope. The inset is a detailed enlargement of the response curve, showing the laser modulation.

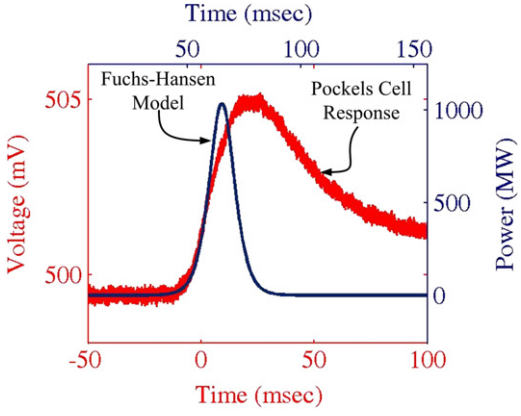

Fig. 8. A comparison of the Fuchs–Hansen model to the EO detector pulse response. Both are plotted on the same time-scale over 150 ms.

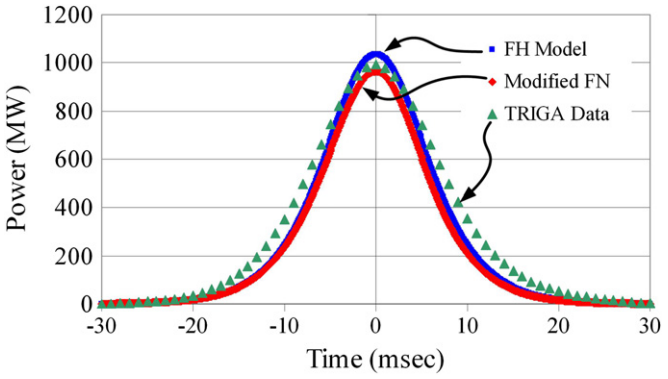

Fig. 9. A comparison power as a function of time of the Fuchs–Hansen (FH), modified Fuchs–Nordheim (FN), and TRIGA reactor data.

Further, the pulses measured with the high sample rate oscilloscope agree well with pulses measured with the Keithley 6485 electrometer and LabView computer program. These results further confirm that the pulses measured with electrometer were accurate, and pulses were not inadvertently missed as a consequence of the relatively long time periods between sample points (10 ms). Also, note that the inset in Fig. 7 shows the 'noise' of the EO detector response was primarily from laser modulation and not random fluctuations of the EO detector electronics.

Note that the magnitude of change in photodiode current for both configurations at the lower bias 1/4 wave setting is larger than the change in photodiode current for the 3/4 wave setting. The bias at the 1/4 wave setting ranges between 1000 to 750 V lower than the 3/4 wave bias setting. Due to lower charge carrier velocities, these lower bias voltages allow the free charge carriers generated from radiation interactions to remain in the crystal for a longer period of time. For higher voltage biases, the free charge carriers will be removed quicker, and, consequently, result in an electric field perturbation of shorter time duration. Ultimately, a smaller change in photodiode current is measured for the higher velocity free charge carriers.

The FWHM of the EO detector response is longer than the theoretical FWHM, most likely due to the location of the detector. The theoretical calculations are for the FWHM of a pulse as observed in the core of the reactor. The EO detector is located approximately six feet away from the reactor exterior, in which neutrons must pass through the moderators (water and then a graphite reflector ring). Thus, neutrons diffuse from the core of the reactor and scatter through water, a graphite reflector, and some biological-shielding, before entering the CZT crystal. Hence, it is expected that the FWHM of the pulse, measured outside of the beam port, is longer than observed in the core.

The EO detector was previously calibrated to fit the height of the pulse and can accurately measure and predict other excess

Table 2
The peak power and FWHM of the FN and FH power excursion models and TRIGA.

Method	Peak power (MW)	FWHM (ms)
Modified FN	965	13.1
FH	1009	13.1
TRIGA	992	16

reactivity insertions [21]. The detector is inaccurate at measuring the FWHM of the pulse as shown in Fig. 8, due to the location of the detector and the charge carrier sweep-out times as previously discussed. However, the peak powers are well calibrated and further supported by the comparison of the theoretical modified Fuchs–Nordheim and Fuchs–Hansen models to the real-time TRIGA data, as shown in Fig. 9. The models also accurately predict the FWHM of the pulse and are on the same order of magnitude.

Finally, because no change in photodiode current was observed using the borated HDPE/Pb shutter nor with the laser powered off, it can be concluded the change in photodiode current is from radiation interactions in the crystal. Furthermore, when using the $LiNbO_3$ crystal, still no change was observed due to the short lifetime of the free carriers in the crystal even when the reactor power was increased more than three orders of magnitude from steady-state operation to pulsing.(Table 2)

6. Conclusions

The CdZnTe Pockels cell has been shown to successfully trace, in real time, nuclear reactor pulses using both a standard and inverted Pockels cell configuration. These results demonstrate, for the first time, successful measurements of a nuclear reactor pulse using an EO radiation detector. CdZnTe, to date, has shown to be the most promising crystal for EO radiation detection, most likely due to the relatively long charge carrier lifetimes as compared to traditional EO crystals (such as $LiNbO_3$). Additional experiments showed the response to be directly resultant from ionizing radiation in the crystal and not electronic noise or scattered radiation.

Acknowledgements

This work was supported in part by DOE NEER contract DE-PS07-03ID14540. The authors express their gratitude to the KSU TRIGA Mark II nuclear reactor staff for their helpful assistance.

References

[1] K.A. Nelson, N. Edwards, M.J. Harrison, A. Kargar, W.J. McNeil, R.A. Rojeski, D.S. McGregor, Nuclear Instruments and Methods A 620 (2010) 363.
[2] M.A. Hossain, E.J. Morton, M.E. Ozsan, IEEE Transactions on Nuclear Science **49** (2002) (1960).
[3] S.F. Mughabghab and D.I. Garber, Neutron Cross Sections, 3rd Ed., BNL-325 Report, Vol. 1 Brookhaven National Laboratory, Upton, 1976.
[4] D.I. Garber and R.R. Kinsey, Neutron Cross Sections, 3rd Ed., BNL-325 Report, Vol. 2 Brookhaven National Laboratory, Upton, 1976.
[5] E.M. Baum, H.D. Knox, T.R. Miller, Nuclides and Isotopes, 16th edn. 2002.
[6] M.A. Lone, R.A. Leavitt, D.A. Harrison, Atomic Data and Nuclear Data Tables **26** (1981) 511.
[7] J.K. Tuli, Thermal Neutron Capture Gamma Rays, BNL-NCS-51647 Report, UC-34-C, Brookhaven National Laboratory 1983.
[8] R.S. Stone, H.P. Sleeper, R.H. Stahl, G. West, Nuclear Science and Engineering **6** (1959) 255.
[9] IAEA Education and Training in Nuclear Safety, TRIGA reactor characteristics, Asian Nuclear Safety Network, 2006.
[10] D. Olander, E. Greenspan, H.D. Garkisch, B. Petrovic, Uranium-zirconium hydride fuel properties, Nuclear Engineering and Design 239 (2009) 1406–1424.
[11] K.A. Terrani, J.E. Seifried, D.R. Olander, Transient hydride fuel behavior in LWRs, Journal of Nuclear Materials 392 (2009) 192–199.
[12] M.T. Simnad, F.C. Foushee, G.B. West, Fuel elements for pulsed TRIGA research reactors, Nuclear Technology 28 (1976) 31–56.
[13] M. Ravnik, Reactor Physics of Pulsing: Fuchs–Hansen Adiabatic Model, ⟨http://www.rcp.ijs.si/ric/pulse_operation-a.html⟩, 2004.
[14] A. Petrovic, M. Ravnik, Phyical model of reactor pulse, Nuclear Energy for New Europe, Portoroz, Slovenia (2004).
[15] G.I. Bell, S. Glasstone, Nuclear Reactor Theory, R.E. Krieger Publishing Co., Inc., Malabar, Florida, 1985.
[16] D.L. Hetrick, Dynamics of Nuclear Reactors, University of Chicago Press, Chicago, 1971.
[17] R.E. Mikesell, GA-1695 (Rev. 5) General Atomics Corp., 1966.
[18] GA-2627 (Rev.), General Atomics Corp., 1964.
[19] M.T. Simnad, Report E-117-833, General Atomics Corp., 1980.
[20] R. Gerson, J.F. Kirchoff, L.E. Halliburton, D.A. Bryan, Journal of Applied Physics **60** (1986) 3553.
[21] K.A. Nelson, J.A. Geuther, J.L. Neihart, T.A. Riedel, R.A. Rojeski, J.L. Saddler, A.J. Schmidt, D.S. McGregor, Applied Radiation and Isotopes, 2012, doi: 10.1016.

Nuclear Instruments and Methods in Physics Research A 690 (2012) 125

Contents lists available at SciVerse ScienceDirect

Nuclear Instruments and Methods in Physics Research A

journal homepage: www.elsevier.com/locate/nima

Erratum

Erratum to "Nuclear reactor pulse tracing using a CdZnTe electro-optic radiation detector" [Nucl. Instr. and Meth. A 680 (2012) 97–102]

Kyle A. Nelson [a,*], Jeffrey A. Geuther [b], James L. Neihart [a], Todd A. Riedel [a], Ronald A. Rojeski [c], Philip B. Ugorowski [a], Douglas S. McGregor [a]

[a] S.M.A.R.T. Laboratory, Mechanical and Nuclear Engineering, Kansas State University, Manhattan, KS 66506, USA
[b] TRIGA Mark II Nuclear Reactor, Mechanical and Nuclear Engineering, Kansas State University, Manhattan, KS 66506, USA
[c] Nanometrics, Inc., 1550 Buckeye Drive, Milpitas, CA 95035, USA

Unfortunately, during the publishing process some errors have been inserted in the article, without the authors knowing it. We have listed below the corrections:

(1) The email address nuclearengg@gmail.com should have been deleted.
(2) In the right column on page 98, fourth paragraph, the constant K needs to be defined. The sentence should read, "…during a pulse can also be calculated using Eq. (5), assuming the reciprocal heat capacity, K, is constant."
(3) Eq. (3) should read:

$$P(t)_{FN} = \frac{NC_p(t)(\rho_{FN}\beta)^2}{2\alpha l}\mathrm{sech}^2\left(\frac{t\rho_{FN}\beta}{2l}\right)$$

(4) In the left column on page 99, second line down, the l should be italicized.
(5) In Table 1, fuel is spelled incorrectly in the description of N.
(6) At the end of the first paragraph on page 102, the following sentence should be added, "The peak powers and FWHM's of the modified Fuchs-Nordheim, Fuchs-Hansen, and TRIGA data are listed in Table 2."

We apologize to the author and to the readers for any confusion that these mistakes may have caused.

DOI of original article: http://dx.doi.org/10.1016/j.nima.2012.02.048
* Corresponding author.
E-mail address: knelson1@ksu.edu (K.A. Nelson).

http://dx.doi.org/10.1016/j.nima.2012.07.050